GSC Biological and Pharmaceutical Sciences
eISSN: 2581-3250 CODEN (USA): GBPSC2
Cross Ref DOI: 10.30574/gscbps
Journal homepage: https://gsconlinepress.com/journals/gscbps/

(RESEARCH ARTICLE)

Secondary metabolites of Euphorbia pulcherrima as Carbonic Anhydrases and Acetylcholinesterase inhibitors: An *in silico* approach

Jesus Alberto Rojas-Morales [1, 2], Jesús Sandoval-Ramírez [3] and Alan Carrasco-Carballo [1, 2, 4, *]

[1] *Laboratory of Elucidation and Synthesis in Organic Chemistry, HJB, VIEP, BUAP, Puebla, Pue., México.*
[2] *Multidisciplinary Laboratory of Biomedicine, Biotechnology and Integrative Bioinformatics applied to Health, FCS UATx, Zacatelco, Tlaxcala.*
[3] *Faculty of Chemistry, BUAP, Puebla, Pue., México.*
[4] *SECIHTI, LESQO, HJB, VIEP, BUAP, Puebla, Pue., México.*

GSC Biological and Pharmaceutical Sciences, 2026, 36(01), 009-021

Publication history: Received on 17 May 2026; revised on 25 June 2026; accepted on 27 June 2026

Article DOI: https://doi.org/10.30574/gscbps.2026.36.1.0241

Abstract

Euphorbia pulcherrima, a member of the Euphorbiaceae family remains a subject of limited exploration concerning its potential medicinal applications. Despite being widely cultivated for ornamental purposes and having ethnomedicinal uses, the comprehensive study of its therapeutic potential is remarkably scarce. This research employs an in *silico* approach to deepen the medicinal properties of secondary metabolites from *E. pulcherrima*. Using structural analysis with the SwissTargetPrediction platform and molecular docking, we have unveiled potential biological targets, including Acetylcholinesterase (AChE) and multiple Carbonic Anhydrase (CA) isoforms, and evaluating Absorption, Distribution, Metabolism, Excretion, and Toxicity (ADMETX) properties to predict the potential uses of this secondary metabolites as bioactive molecules. Our findings suggest that several molecules related to hydroxybenzoic acid demonstrate significant inhibitory potential against not only AChE but also three distinct CA isoforms suggesting the potential utility of *E. pulcherrima* secondary metabolites in combating diseases related to these enzymatic targets, such as Alzheimer's disease. In conclusion, this research shows the therapeutic possibilities residing within the secondary metabolites of *E. pulcherrima*. It underscores the importance of further investigation and validation of these bioactive compounds for their potential role in modern medicine, promising new avenues for drug development and innovative approaches to addressing various human diseases.

Keyboards: Euphorbia Pulcherrima; Structural Comparison; Molecular Docking; In Silico Approach

1. Introduction

Euphorbia pulcherrima, commonly known in México as “Flor de Nochebuena” (Christmas Eve flower) or poinsettia, is one of the most emblematic and economically important ornamental plant that belongs to the family Euphorbiaceae, characterized to produce a white latex and include about 1600 species distributed in tropical and subtropical areas worldwide [1,2]. Despite being primarily utilized as an ornamental plant, this flower presents ethnomedicinal uses in México due to the presence of terpenoids, flavonoids and steroids, some of which present well-known potent and diverse biological activity (Figure 2) as Euphorbiaceae family members stand for treatment of skin diseases, migraine, or intestinal parasites [3–5].

* Corresponding author: Alan Carrasco-Carballo

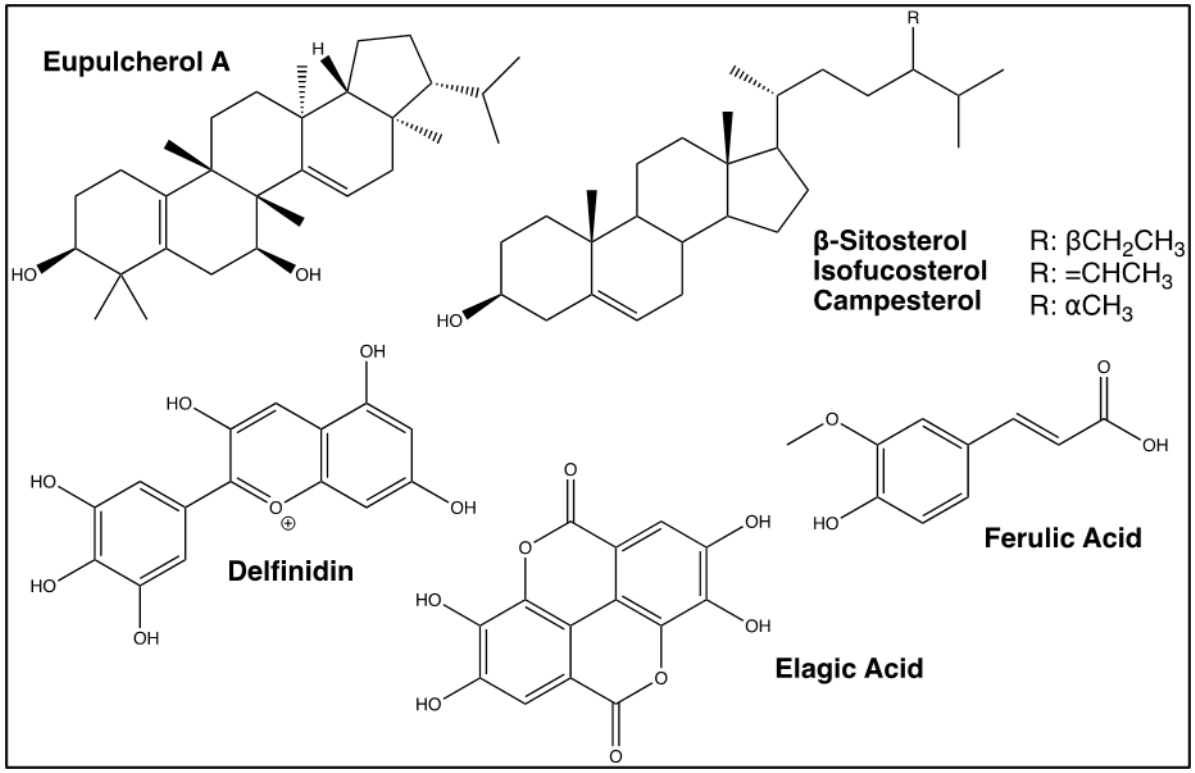

Figure 1 Chemical structure of some secondary metabolites in *E. pulcherrima* (2–5]

Molecular docking has been proven to be a useful tool to predict the potential of a variety of compounds, especially those present as secondary metabolites in plants where a classical focus of isolating (Figure 1), purifying, and evaluating *in vitro* or *in vivo* is time-and-money-costing. With the use of *in silico* approaches, researchers are capable of evaluating high quantities of molecules against a battery of biological targets and determining their potential uses as part of medicinal plants [6]. Plant-derived secondary metabolites could present beneficial uses against human diseases where *in silico* studies can reveal potential biological targets; examples of this approach can be seen in the studies against the pandemic SARS-CoV 2 [7], cancer-associated targets [8], myeloproliferative neoplasias [9] , and as antimicrobials [10].

The scope of this paper is to analyse the potential biological activities of secondary metabolites from *Euphorbia pulcherrima* as inhibitors of carbonic anhydrases and acetylcholinesterase using an *in silico* approach involving molecular docking and prediction of their ADMET properties.

2. Material and methods

2.1. Hardware and Software

The hardware used was a PC with Windows 11 Pro-64bit, an Intel® CoreTM i9-10900 RAM 64.00 GB @ 2.80 GHz, ChemDraw Professional suite 17.1 were used to obtain SMILES (www.3ds.com/). SwissTargetPrediction platform was used to predict biological targets with a probability of interaction (http://www.swisstargetprediction.ch/) [11]. Preparation of secondary metabolites ligands, substrates and reference drugs was designed using Maestro software from the Schrödinger platform, minimized with Macromodel [12] and optimized to physiological conditions in LigPrep [13] according to the previously reported methodology [14]. Proteins were prepared in the Protein-Preparation-Wizard module [15] from the Schrödinger platform under physiological conditions according to the previously reported methodology [14]. Molecular docking was performed using Schrodinger's Glide module [16]. The prediction of ADMETx properties was made in the QikProp module [17] of the Schrödinger platform, and the mean lethal dose was predicted by the GUSAR platform [18] according to the SMILES of each structure.

2.2. Ligands

The obtained structures were obtained through bibliographical revision and compared to entries from PubChem or research articles: 25 secondary metabolites reported from *E. pulcherrima* were evaluated: β-sitosterol (PubChem ID: 222284), Caffeic Acid (689043), Campesterol (173183), Chlorogenic Acid (1794427), Cholesterol (5997), Cyanidin

(128861), Cycloart-23-ene diol (5470009), Cycloart-25-ene diol (11419367), Dihydrobrassicasterol (5283637), Delfinidin (25203213), Ellagic Acid (5281855), Eupulcherol A (Ref: 2), Ferulic Acid (445858), Galangin (5281616), Gallic Acid (370), Isofucosterol (5281326), Kaempferol (5280863), Myricetin (5281672), *p*-coumaric acid (637542), Patuletin (5281678), Phloretin (4778), *p*-hydroxibenzoic acid (135), Quercetin (5280343), Spinacetin (5321435), Stigmasterol (5280794), Syringic acid (10742), Vanillic acid (8468), Testosterone (6013), Letrozole (3902), DHT (10635), Flutamide (3397), Estradiol (5757), Tamoxifen (2733526), Raloxifen (46882308), 4KM (91827511), Acetylcholine (187), Metrifonate (5853), Ethoxzolamide (3295), BL0 (23653536), Acetazolamide (1986), Chlorthalidone (2732), L8N, Indapamide (3702)

2.2.1. Receptors

The receptors used as the molecular targets were: Steroid associated: Androgen Receptor (PDB ID: 2PIQ) [19], Cytochrome P450 19A1 (PDB ID: 3EQM) [20], Estrogen Receptor isoforms α and β (PDB ID: 1A52 and 5TOA, respectively) [21,22] and Liver X Receptor α (PDB ID: 5AVI) [23]. Central Nervous system associated: Acetylcholinesterase (PDB ID: 4M0E) [24] and Butyrylcholinesterase (PDB ID: 7AIY) [25]. Carbonic Anhydrases: Isoforms I, II, III, IV, VII, IX, XII, XIII (PDB IDs: 3LXE, 3BL0, 1Z97, 3FW3, 6SDT, 5FL4, 4QJ0, 4QIZ, respectively) [26–32]; all of them retrieved from the Protein Data Bank (https://www.rcsb.org/)

2.3. Docking protocol

Molecular docking was performed using Schrödinger's Glide module [16) in XP mode, with flexibility on the site according to the previously reported methodology [14]. All proteins were validated with their co-crystal, obtaining RMSD values less than 2.0 Å in each case.

2.4. Assessment

The selection of proteins was carried out according to the quality of each crystal. Docking scores (DS) were compared between secondary metabolites and reference molecules: Endogenous substrates/ligands or a reference drug, if available.

3. Results and Discussion

3.1. Target prediction of secondary metabolites

The structural-based biological target prediction by the Swiss Target Prediction Platform (STP) returned 291 targets with at least 1 interaction with the evaluated molecules including enzymes and nuclear receptors; accordingly, with the highest frequency of interaction targets (Figure 2), the selection criteria of ≥40% was applied and 13 proteins were selected including steroid-associated proteins: Estrogen receptor isoform α and β, and aromatase (ERα, ERβ, CYP19A1); carbonic anhydrases: (CA, 7 isoforms) and acetylcholinesterase (AChE) a protein related to central nervous system (CNS).

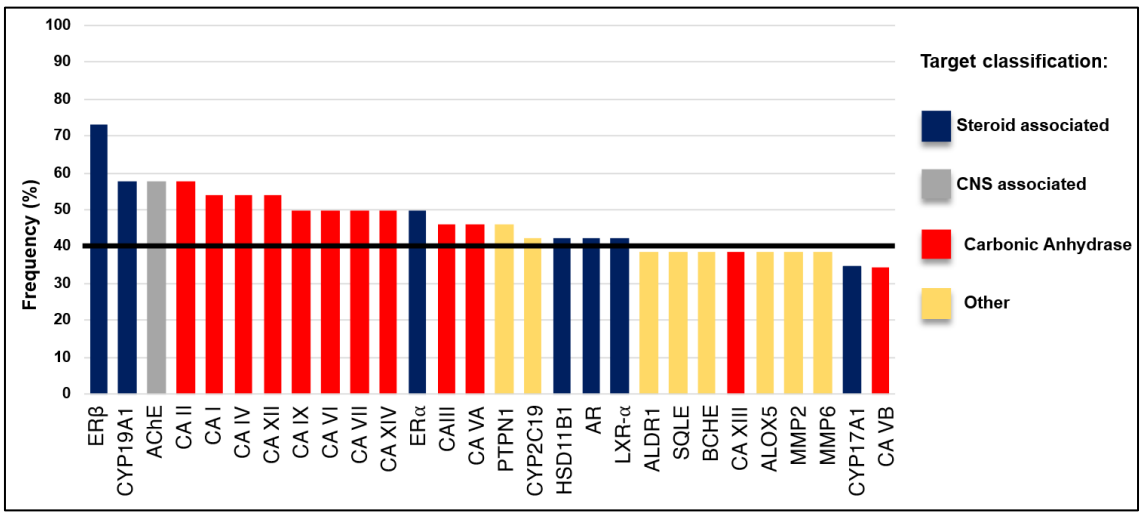

Figure 2 Percentage frequency diagram of *Euphorbia pulcherrima* secondary metabolites targets by STP. The cut-off point was chosen at 40% to include most of the 3 main classes of targets obtained

The *in silico* protein prediction in this study paves the way for various applications based on their bibliographic reports. However, a structural comparison analysis could suggest the likelihood of interaction. To advance this research, the next step involves conducting molecular docking studies, aligning the metabolite database with the corresponding proteins, and comparing them with their reference ligands/substrates, as well as commercially available drugs.

To determine if secondary metabolites of *E. pulcherrima* have medicinal potential against the selected targets, docking score values were obtained by molecular docking on Glide and comparing them with reference inhibitors. Among the only 5 steroid-associated proteins (previously obtained by STP), only CYP19A1 exhibited significant docking score, conversely, several molecules demonstrated higher DS compared to the reference inhibitors in CA targets and AChE.

3.2. Molecular docking on steroid-associated proteins

Of the steroid-associated proteins, we observed that in most of the cases, the structures were capable to fit in the active site of all the steroidal-associated structures (Figure 3), however, their DS were insufficient to be considered as inhibitors in comparison to the DS values of their endogenous substrates (Table I).

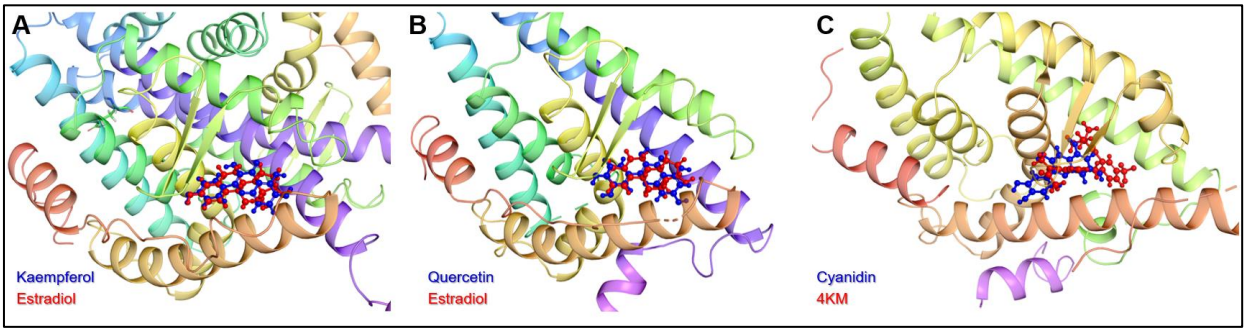

Figure 3 Superposition of structures and endogenous ligands in the active sites of the steroidal receptors: A) ERα, B) ERβ and C) LXR-α

This can be explained by the nature of the secondary metabolites found in *E. pulcherrima* most characterized for their aromatic moieties, and in the case of the steroid-like metabolites, they are far larger than the endogenous ligands of the sexual hormone binding receptors or enzymes.

Table 1 Docking scores of metabolites with steroidal-associated proteins

Molecule	CYP19A1	AR	ERα	ERβ	LXR-α
β-sitosterol	NI	-1.736	NI	NI	-8.705
Caffeic Acid	-5.443	-3.239	-6.396	-6.955	-6.069
Campesterol	NI	-1.655	NI	NI	-8.296
Chlorogenic Acid	-5.443	-3.907	-6.133	-4.073	-7.588
Cholesterol	NI	-1.702	NI	NI	-9.203
Cyanidin	-8.111	-4.063	-8.648	-5.291	-9.223
Cycloart-23-ene diol	NI	-3.545	NI	NI	-8.021
Cycloart-25-ene diol	NI	-2.562	NI	NI	-8.988
Dehydrobrassicasterol	NI	-1.61	NI	NI	-8.619
Delfinidin	-8.127	-4.263	-5.786	-5.513	-9.203
Ellagic Acid	-8.133	-3.979	-7.947	-4.054	-5.237
Eupulcherol A	NI	-2.125	NI	NI	NI
Ferulic Acid	-5.453	-3.145	-5.639	-4.123	-5.723

Galangin	-8.427	-3.723	-7.303	-8.251	-8.517
Galic Acid	-5.58	-4.527	-6.351	-6.922	-6.705
Isofucosterol	NI	-1.57	NI	NI	-8.882
Kaempferol	-5.819	-4.327	-8.994	-9.417	-7.744
Myricetin	-7.61	-3.559	-3.959	-5.393	-7.494
p-coumaric acid	-4.731	-3.142	-6.021	-6.199	-5.118
Patuletin	NI	-4.2	-4.926	-4.614	-7.951
Phloretin	-7.701	-3.257	-8.025	-8.479	-7.753
p-hydroxibenzoic acid	-5.833	-4.528	-6.216	-6.204	-6.298
Quercetin	-8.729	-3.611	-7.955	-9.078	-8.303
Spinacetin	-4.432	-3.641	-6.043	-4.664	-8.435
Stigmasterol	NI	-1.752	NI	NI	-8.84
Syringic acid	-5.943	-4.135	-5.923	-4.173	-6.329
Vanillic acid	-5.856	-4.215	-5.676	-5.019	-7.515
Testosterone^{+}	-10.383	-	-	-	-
Letrozole^{++}	-6.256	-	-	-	-
DHT^{+}	-	-11.129	-	-	-
Flutamide^{++}	-	-7.259	-	-	-
Estradiol^{+}	-	-	-10.38	-10.013	-
Tamoxifen^{++}	-	-	-9.326	-	-
Raloxifen^{++}	-	-	-	-9.559	-
4KM^{++}	-	-	-	-	-10.494

NI: No Interaction, $^{+}$: Endogenous substrate/ligand, $^{++}$: Principal drug of reference

Compared to the commercial non-steroidal inhibitor letrozole, 6 compounds with aromatic moieties showed greater DS with the reference inhibitor as shown below in the case of CYP19A1 whereas in the case of flavonoids showed strong interactions both with the heme group and residues in the catalytic site (Figure 4). The principal interactions of letrozole, a commercial inhibitor for CYP19A1 (also known as aromatase) in the active site involve salt bridges between the triazole ring and the Fe^{2+} atom along with an additional interaction with Trp224 as a π-π stacking interaction showing that the interaction with the heme group is essential for the inhibition of the enzyme (Figure 5A). However, the interactions present in the endogenous substrate testosterone (T) exhibit an H-bond between Met374 and the 17β-hydroxyl group of testosterone, a crucial interaction in the catalytic activities of the enzyme; (Figure 5A y 5B); its higher affinity for the active site is explained due to the presence of aliphatic sites that are more compatible with the hydrophobic nature of T in comparison of the highly polar nitrile groups of letrozole. Suggesting that these metabolites do have not the potential to disrupt endocrinal pathways associated with steroidal hormones.

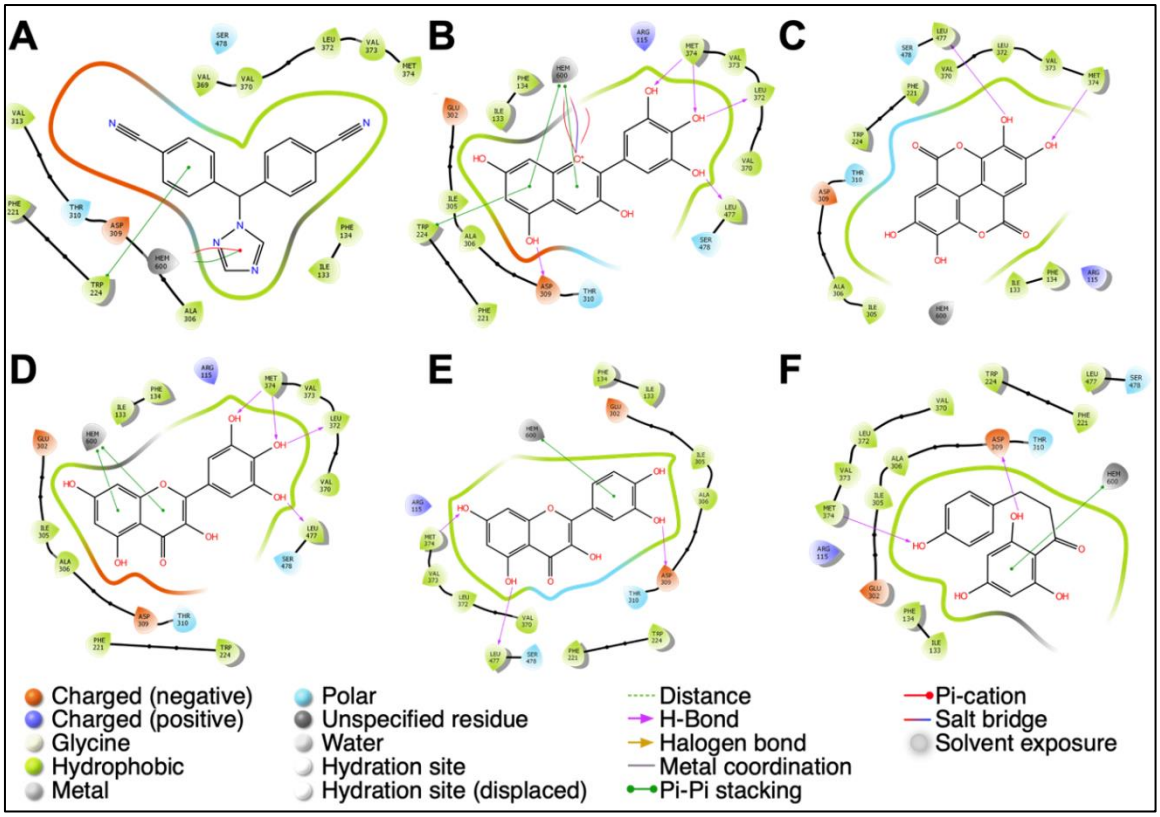

Figure 4 Potential CYP19A1 inhibitors and their 2D structural interactions, between A) Letrozole B) Delfinidin C) Ellagic acid D) Myricetin E) Quercetin F) Phloretin

In the case of the anthocyanidins delphinidin (Figure 4B) and cyanidin, the principal interactions occur in the oxonium ion and the heme group and additional π-π stacking interactions with the aromatic rings of the flavylium ion, however, the number of hydroxyl substituents affects the DS obtained, in the case of delphinidin (with a tri-hydroxy substituted aromatic ring in C2), with 4 H-bonds between Leu477, Leu372 and Met374 and showing DS -0.017 kcal/mol superior to cyanidin with only two hydroxy-substituted aromatic ring and 3 H-bonds (Leu372 and Met374). It can also be seen in the other molecules that hydrogen bonds are essential for strong interactions in the active sites. Notably, in the case of quercetin, the absence of a salt bridge between the heme group is compensated for by the H-bond interactions resulting in the highest DS obtained of all the molecules evaluated (Figure 4E). This finding suggests that these molecules have the potential to be outstanding competitive inhibitors of CYP19A1, thereby aiding in the modulation of the enzymatic activity.

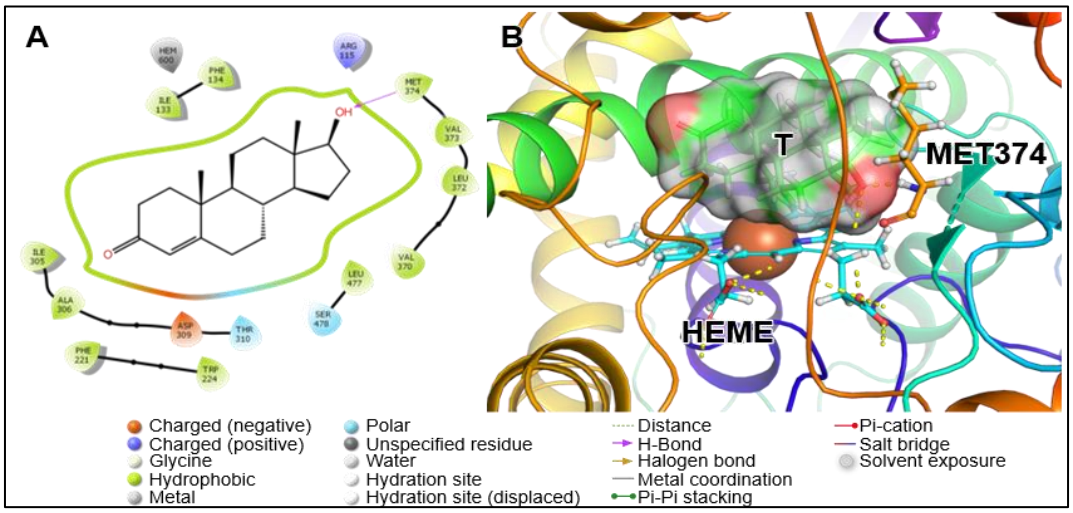

Figure 5 2D structure showing the polar surface of active site and 3D structure interaction of testosterone.

3.3. Molecular docking on Central Nervous System enzymes

Acetylcholinesterase, a critical enzyme in CNS plays a pivotal role in the hydrolysis of acetylcholine into choline and acetate ions. It serves as the primary target in the treatment of Alzheimer's disease increasing Acetylcholine levels. The search for novel reversible inhibitor drugs of this enzyme aims to preserve acetylcholine levels in different areas of the CNS and would be useful in the treatment of this pathology. Our results show that *p*-hydroxybenzoic, syringic and vanillic acid are the only molecules capable of fitting the active site of AChE; phloretin showed the highest DS of all the metabolites studied (Figure 6), however, a detailed revision disclosed that this molecule is not near of the active site, therefore only molecules situated in active site were analysed.

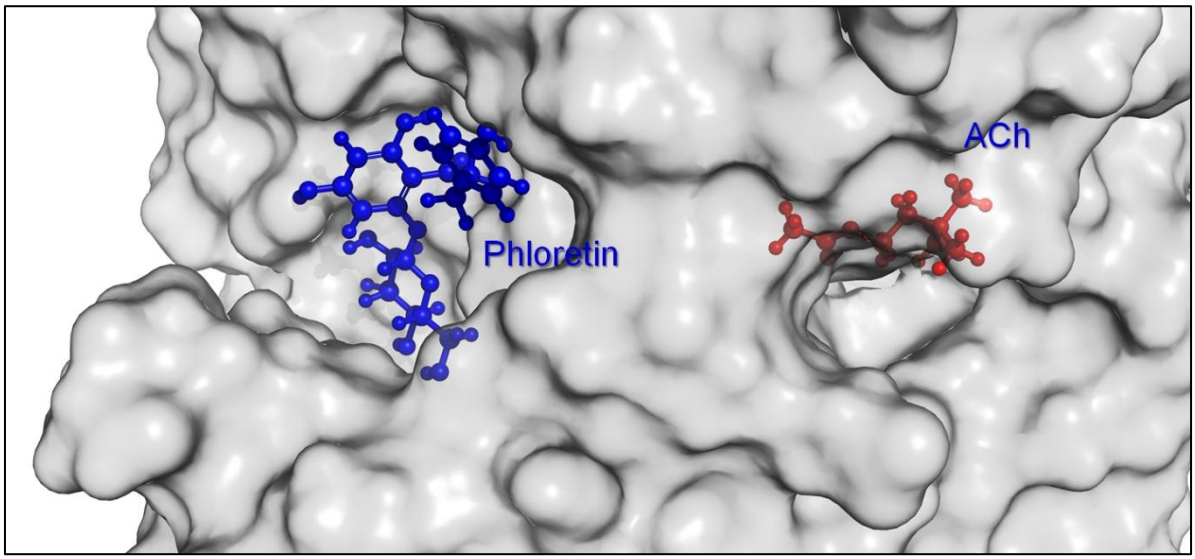

Figure 6 3D Surface of AChE showing ACh in its active site and Phloretin in a cavity.

Table 2 Docking score of metabolites with CNS-associated proteins

Molecule	DS	Molecule	DS	Molecule	DS
β-sitosterol	NI	Ellagic Acid	NI	Phloretin	-7.150
Caffeic Acid	-4.843	Eupulcherol A	NI	*p*-hydroxibenzoic acid	-6.209
Campesterol	NI	Ferulic Acid	-5.373	Quercetin	NI
Chlorogenic Acid	NI	Galangin	NI	Rutin	-4.543
Cholesterol	NI	Galic Acid	-4.275	Spinacetin	NI
Cianylattdin	NI	Isofucosterol	NI	Stigmasterol	NI
Cycloart-23-ene diol	-4.372	Kaempferol	NI	Syringic acid	-5.982
Cycloart-25-ene diol	-4.185	Myricetin	NI	Vanillic acid	-6.036
Dehydrobrassicasterol	NI	*p*-coumaric acid	-4.354	Acetylcholine	-3.546
Delfinidin	NI	Patuletin	NI	Metrifonate	-5.506

NI: No interaction

The nature of the active site of AChE has been exhaustively studied, where the "catalytic triad" is located near the bottom of a deep and narrow recognized cavity conformed of well-conservated 14 aromatic residues, being subject to inhibition for potential molecules [24]. The molecules with the greatest docking score were hydroxybenzoic acids; *p*-hydroxybenzoic acid presents an H-bond between a Glh202 and the carboxylic acid fraction of the molecule. Additionally, and due to the aromatic nature of the compound, we can observe a π-π stacking interaction mediated by the aromatic rings of the ligand and Tyr337 of AChE, which makes it have a greater docking score (Figure 7B).

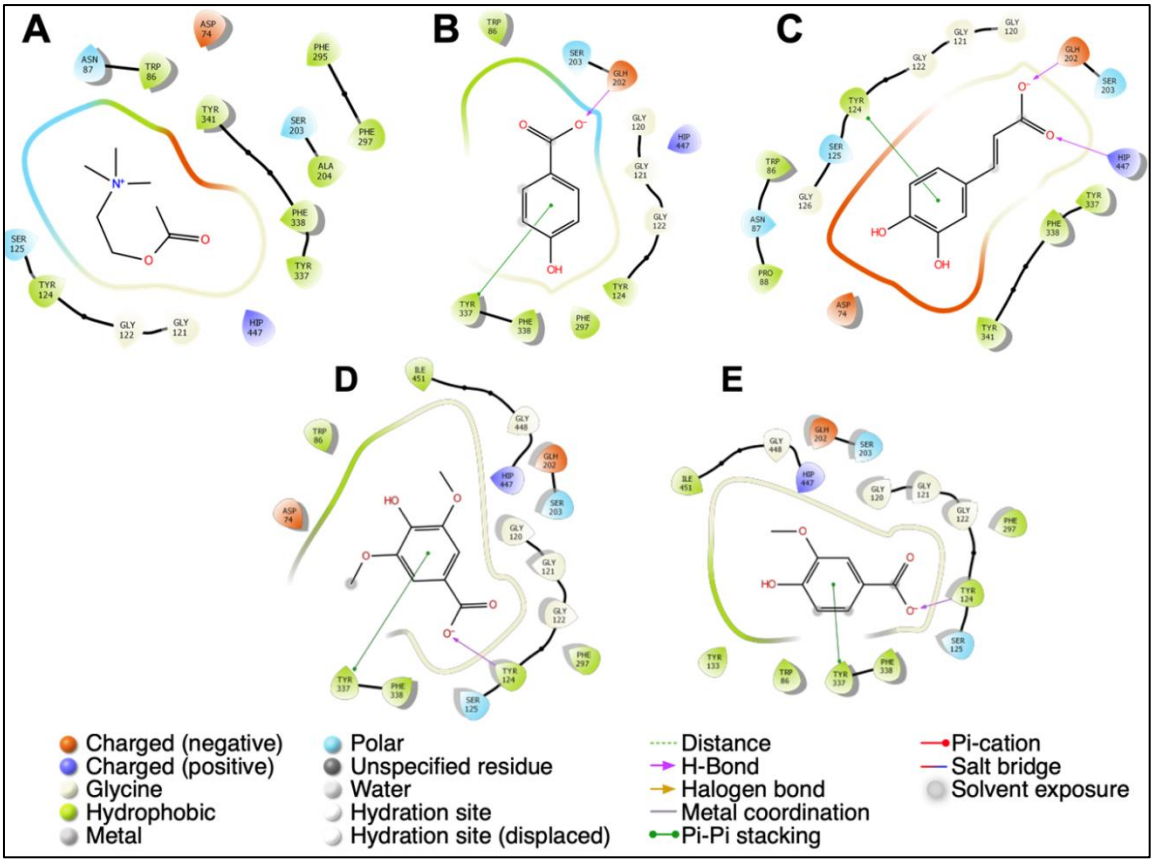

Figure 7 Structures that possibly interact with AChE. A) Acetylcholine (ACh), B) *p*-Hydroxybenzoic acid, C) Caffeic acid, D) syringic acid and E) Vanillic acid

In the case of vanillic acid, the carboxylic acid interacts directly with Tyr124 changing the position in comparison with *p*-hydroxybenzoic acid and now situating the hydroxyl and ester groups near Glh202 but conservating the π-π stacking interaction with Tyr337 (Figure 8 E) suggesting a conventional blockage of the active site.

On the other hand, due to its larger size, caffeic acid (Figure 8 E) has an antioxidant effect due to its aromatic structure, double bonds, and hydroxyl groups. In addition, H bond interactions between the protonated Glh202 and Hip447 and the carboxylic acid of this molecule and a π-π stacking interaction with Tyr124; Negatively charged interactions also occur between the vicinal hydroxyl of the aromatic ring and Asp74, suggesting electrical repulsions that explain the lack of a better ECB despite the number and strength of the interactions. Similar interactions can be found in the rest of the molecules that showed higher DS. All these interactions make caffeic acid useful in cancer diseases and Alzheimer's disease.

Similar interactions can be found in the rest of the molecules that showed superior DS of the substrates and drugs of reference indicating that this class of secondary metabolites of *E. pulcherrima* could be useful in the treatment of neurodegenerative diseases associated with AChE.

3.4. Molecular docking on Carbonic Anhydrases isoforms

Carbonic anhydrases are ubiquitous metalloenzymes that catalyse the hydration of carbon dioxide with the ability to modify cellular pH and influence cellular proliferation, migration, and invasion, especially in malignant tissues and another variety of processes such as CO_2 transport at lungs, acidic and alkaline enteral secretions, cerebrospinal fluid, and aqueous humour.

Molecular docking of the secondary metabolites showed that despite structural comparison suggesting potential activity with 8 carbonic anhydrases, only 3 of them had superior DS compared to their known inhibitors and were in the active site. Syringic acid, a phenolic acid that exhibits multi-pharmacologic properties was a common denominator in the three carbonic anhydrases, this can be attributed to the structural similitude with the endogenous substrate HCO_3^- .

Table 3 Docking score of metabolites with Carbonic anhydrase enzymes

Molecule	**CAI**	**CAII**	**CAIII**	**CAIV**	**CAVII**	**CAIX**	**CAXII**	**CAXIII**
β-sitosterol	NI	-3.601	NI	-2.764	NI	-4.55	-2.374	-2.836
Caffeic Acid	-4.937	-7.481	-3.573	-7,391	-4.012	-4.789	-3.744	-5.171
Campesterol	NI	-2.735	NI	NI	-2.389	-4.786	-2.695	-3.405
Chlorogenic Acid	-5.598	-4.121	0.226	-5.047	NI	-6.171	-3.453	-6.21
Cholesterol	NI	-3.624	NI	-2.564	NI	-5.4	-2.998	-3.631
Cianydin	-6.361	-5.173	-2.417	-5.978	-5.663	-8.417	-5.99	-5.643
Cycloart-23-ene diol	-3.613	-3.199	NI	-3.187	-4.03	-5.184	-2.839	-3.941
Cycloart-25-ene diol	NI	-3.597	NI	NI	-3.475	-4.881	-3.02	-4.821
Dehydrobrassicasterol	NI	-2.687	NI	NI	-2.448	-5.338	-2.406	-3.674
Delfinidin	-5.732	-5.098	-2.472	-5.668	NI	-8.513	-6.006	-5.429
Ellagic Acid	-5.084	-6.556	-3.95	-6.893	-6.17	-5.954	NI	-4.182
Eupulcherol A	NI	NI	NI	NI	NI	-5.083	-2.307	NI
Ferulic Acid	-5.637	-7.719	-4.013	-7.53	-6.563	-4.748	-3.375	-4.453
Galangin	-5.227	-5.859	-3.381	-5.715	-2.981	-6.094	-4.26	-4.299
Galic Acid	-5.112	-8.044	-4.425	-8.216	-8.432	-5.485	NI	-6.636
Isofucosterol	NI	-2.978	NI	-3.503	-2.224	-4.781	-2.676	-3.381
Kaempferol	-6.17	-5.933	-2.387	-5.159	-4.991	-6.295	-4.28	-5.202
Myricetin	-5.192	-6.967	NI	-7.425	-4.326	-7.275	-4.045	-4.518
p-coumaric acid	-4.204	-7.203	-4.43	-7.252	-5.483	-4.583	-3.34	-5.252
Patuletin	-5.311	-4.685	NI	-5.101	-4.831	-6.601	-4.777	-4.474
Phloretin	-6.122	-5.519	-5.798	-5.939	-6.039	-6.593	-3.303	-6.082
p-hydroxibenzoic acid	-5.566	-7.848	-5.018	-8.105	-7.812	-5.244	NI	-5.112
Quercetin	-5.558	-5.648	-1.31	-6.128	-3.421	-6.616	-5.038	-4.35
Rutin	-4.152	-3.095	NI	-6.229	-2.632	-9.483	-4.824	-5.901
Spinacetin	-4.706	-4.328	NI	-3.085	-3.574	-7.224	-4.488	-4.139
Stigmasterol	NI	-3.553	NI	NI	NI	-5.789	-2.517	-3.41
Syringic acid	-4.737	-8.947	-4.765	-8.525	-5.265	-5.332	NI	-5.685
Vanillic acid	-5.814	-8.703	-4.665	-8.204	-8.068	-5.319	NI	-5.877
Ethoxzolamide	-5.5							
BL0		-5.25						
Acetazolamide				-6.822				
Chlorthalidone					-6.424			
L8N						-4.197		
Indapamide							-3.108	-3.108

The principal interactions are mediated with metal coordination and a salt bridge between the carboxylate of syringic acid and the metal ion Zn^{2+}.

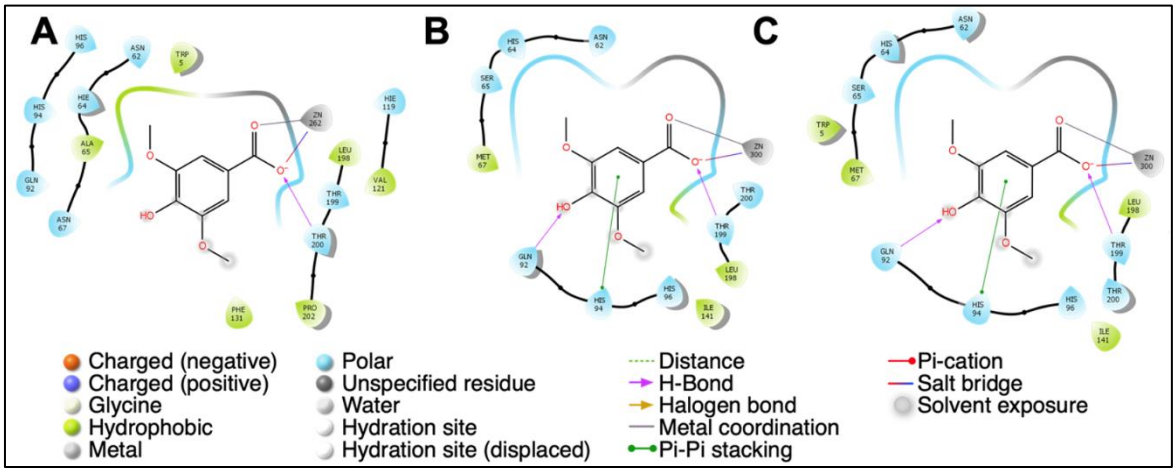

Figure 8 2D-interactions of syringic acid with A) CAII, B) CAIV, C) CAVII

In the case of CAII (Figure 8A), additionally, there is an H-bond between the polar hydrogen of the amide of Thr200 and the carboxylate. On the other hand, in CAIV there are present all the interactions before mentioned, only change to a Thr199 interaction. Another H-bond can be found between polar hydrogens in the amide of the side chain of Gln92 and a stacking interaction with the aromatic imidazole ring of His94 and the aromatic ring of syringic acid, the same interactions that were found in CAVII.

3.5. ADMETx predictions

Secondary metabolites with activity in CNS must not only demonstrate selectivity in their biological targets to be deemed potential drugs but also overcome the primary challenge of effectively penetrating the blood-brain barrier (BBB) with a high lipid solubility that ensures membranes trespassing and present a convenient administration route where oral dosage is the most useful. For all the secondary metabolites evaluated, we found that the most lipophilic compounds (the steroidal ones) presented the highest ratio of oral absorption and QPlogBB, a parameter that estimates the permeability of the compound on BBB (Table 5). The hydroxybenzoic acids that showed the highest DS against AChE presented oral absorptions above 60% and relevant QPlogBB (Figure 9).

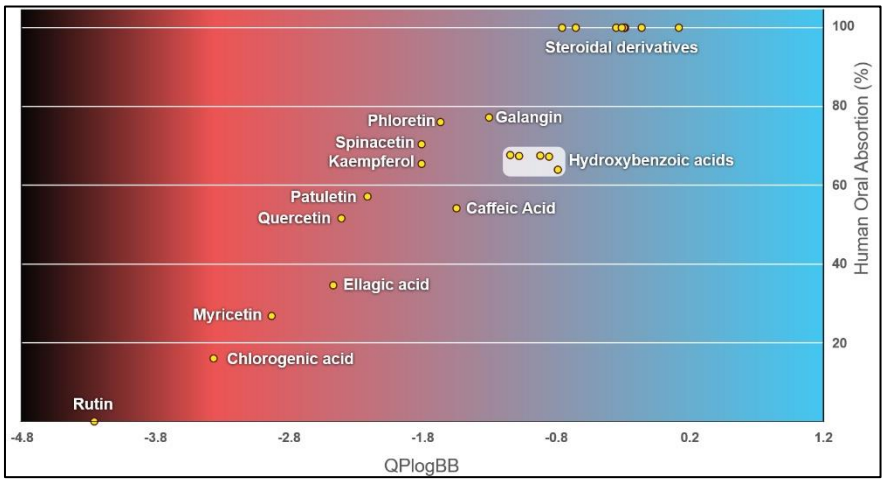

Figure 9 Blood-Brain Barrier permeability parameter (QPlogBB) vs Human Oral Absorption plot

Common perception, particularly in the United States, has often suggested that Poinsettia may pose a toxicological risk. However, this assertion has been widely challenged. To expand the current knowledge and highlight the potential applications in diseases related to AChE and CA, we conducted LD_{50} predictions for the metabolites. The compounds with the highest oral bioavailability showed LD>1000 mg/kg or classified as Class 3: slightly toxic.

Table 4 Predicted LD_{50} to intraperitoneal, intravenous, oral, and subcutaneous routes in rat (mg/kg)

Compound	IP	IV	Oral	SC
β-sitosterol	896.7	5.9	1280.0	838.7
Caffeic acid	890.2	361.4	2386.0	574.7
Campesterol	1190.0	7.0	748.0	1012.0
Chlorogenic acid	1416.0	229.3	3927.0	343.2
Cholesterol	1072.0	11.9	1322.0	1045.0
Cycloart-23-ene diol	937.8	4.7	1213.0	47.4+
Cycloart-25-ene diol	943.7	4.0	758.2	328.4
Dehydrobrassicasterol	1190.0	7.0	748.0	1012.0
Delfinidin	730.8	372.6	1587.0	1983.0
Ellagic Acid	917.2	152.5	1712.0	1927.0+
Eupulcherol A	1078.0	2.8	1182.0	232.4
Ferulic acid	682.3	224.4	2754.0	1058.0
Galangin	815.7	397.6	2737.0	4794.0+
Gallic acid	1144.0	465.9	1606.0	813.7
Isofucosterol	85.3	0.9+	147.9+	760.1
Lupeol	1684.0	5.9	2888.0	786.9
Myricetin	858.5	2376.0+	2227.0	2413.0
Patuletin	780.8	2073.0+	1697.0	3445.0
p-coumaric acid	692.3	303.2	2181.0	578.7
Phloretin	702.2	179.7	1536.0	1232.0
Phlorizin	735.4	1645.0	2127.0	6334.0
p-hydroxybenzoic acid	1081.0	276.3	2291.0	1255.0
Quercetin	920.3	2089.0+	1892.0	3550.0+
Rutin	122.0+	2132.0	2953.0	1653.0
Spinacetin	936.1	1987.0+	2042.0	3388.0
Stigmasterol	786.1	0.8+	62.9+	342.7
Syringic acid	1365.0	248.0	1331.0	1553.0
Vanillic acid	1731.0+	237.6	1725.0	1225.0
Kaempferol	1163.0	392.6	2183.0	5938.0

+ Out of applicability domain of models

4. Conclusion

E. pulcherrima secondary metabolites exhibit a remarkable *in silico* potential to interact with the central nervous system through their interaction with Acetylcholinesterase (AChE). This potential is heightened by their high bioavailability for hydroxy-benzoic acid derivatives able to penetrate the blood-brain barrier effectively. Also, this investigation revealed potential Carbonic Anhydrase (CA) inhibition. Notably, these inhibitors display a low toxicity profile. These findings not only underscore its importance in potential medical applications. Further research and validation are necessary to reveal the full spectrum of its medicinal applications.

Compliance with ethical standards

Disclosure of conflict of interest

The authors have no conflicts of interest.

Funding

This study was financially supported by scholar ship SECIHTI-34462

References

[1] Vasas A, Hohmann J. *Euphorbia* Diterpenes: Isolation, Structure, Biological Activity, and Synthesis (2008–2012). Chem Rev. 2014 Sep 10;114(17):8579–612.

[2] Yu CX, Wang RY, Qi FM, Su PJ, Yu YF, Li B, et al. Eupulcherol A, a triterpenoid with a new carbon skeleton from Euphorbia pulcherrima, and its anti-Alzheimer's disease bioactivity. Org Biomol Chem. 2020;18(1):76–80.

[3] Ernst M, Grace OM, Saslis-Lagoudakis CH, Nilsson N, Simonsen HT, Rønsted N. Global medicinal uses of Euphorbia

[4] Mendioro MS, Diaz MGQ, Alcantara MTB, Hilario OJ, Mateo P, Maghirang RDM. Cytological Studies of Selected Medicinal Plants: Euphorbia pulcherrima Willd. ex Klotz., Moringa oleifera Lam., Catharanthus roseus (L.) Don., and Chrysanthemum indicum Linn. 2005;134(1).

[5] Rauf A, Raza M, Humayun Khan M, Hemeg HA, Al-Awthan YS, Bahattab O, et al. *In vitro* and *in silico* studies on clinically important enzymes inhibitory activities of flavonoids isolated from *Euphorbia pulcherrima*. Annals of Medicine. 2022 Dec 31;54(1):495–506.

[6] Ahmed M, Khan K ur R, Ahmad S, Aati HY, Ovatlarnporn C, Rehman MS ur, et al. Comprehensive Phytochemical Profiling, Biological Activities, and Molecular Docking Studies of Pleurospermum candollei: An Insight into Potential for Natural Products Development. Molecules. 2022 Jun 26;27(13):4113.

[7] Basu A, Sarkar A, Maulik U. Molecular docking study of potential phytochemicals and their effects on the complex of SARS-CoV2 spike protein and human ACE2. Sci Rep. 2020 Oct 19;10(1):17699.

[8] Mendie LE, Hemalatha S. Molecular Docking of Phytochemicals Targeting GFRs as Therapeutic Sites for Cancer: an In Silico Study. Appl Biochem Biotechnol. 2022 Jan;194(1):215–31.

[9] Achutha AS, Pushpa VL, Manoj KB. Comparative molecular docking studies of phytochemicals as Jak2 inhibitors using Autodock and ArgusLab. Materials Today: Proceedings. 2021;41:711–6.

[10] Umesh HR, Ramesh KV, Devaraju KS. Molecular docking studies of phytochemicals against trehalose–6–phosphate phosphatases of pathogenic microbes. Beni-Suef Univ J Basic Appl Sci. 2020 Dec;9(1):5.

[11] Daina A, Michielin O, Zoete V. SwissTargetPrediction: updated data and new features for efficient prediction of protein targets of small molecules. Nucleic Acids Research. 2019 Jul 2;47(W1):W357–64.

[12] Mohamadi F, Richards NGJ, Guida WC, Liskamp R, Lipton M, Caufield C, et al. Macromodel an integrated software system for modeling organic and bioorganic molecules using molecular mechanics. J Comput Chem. 1990 May;11(4):440–67.

[13] Schrödinger Release 2022-3: LigPrep. Scrödinger LLC; 2021.

[14] Carrasco-Carballo A, Mendoza-Lara DF, Rojas-Morales JA, Alatriste V, Merino-Montiel P, Luna F, et al. In silico Study of Coumarins Derivatives With Potential Use in Systemic Diseases. Biointerface Res Appl Chem. 2022 Jun 6;13(3):240.

[15] Schrödinger Release 2022-3: Protein Preparation Wizard. Scrödinger LLC; 2021.

[16] Friesner RA, Banks JL, Murphy RB, Halgren TA, Klicic JJ, Mainz DT, et al. Glide: A New Approach for Rapid, Accurate Docking and Scoring. 1. Method and Assessment of Docking Accuracy. J Med Chem. 2004 Mar 1;47(7):1739–49.

[17] Schrödinger Release 2022-3: QikProp. Scrödinger LLC; 2021.

[18] Filimonov DA, Zakharov AV, Lagunin AA, Poroikov VV. QNA-based 'Star Track' QSAR approach. SAR and QSAR in Environmental Research. 2009 Oct;20(7–8):679–709.

[19] Estébanez-Perpiñá E, Arnold LA, Nguyen P, Rodrigues ED, Mar E, Bateman R, et al. A surface on the androgen receptor that allosterically regulates coactivator binding. Proc Natl Acad Sci USA. 2007 Oct 9;104(41):16074–9.

[20] Ghosh D, Griswold J, Erman M, Pangborn W. Structural basis for androgen specificity and oestrogen synthesis in human aromatase. Nature. 2009 Jan;457(7226):219–23.

[21] Tanenbaum DM, Wang Y, Williams SP, Sigler PB. Crystallographic comparison of the estrogen and progesterone receptor's ligand binding domains. Proc Natl Acad Sci USA. 1998 May 26;95(11):5998–6003.

[22] Souza PCT, Textor LC, Melo DC, Nascimento AS, Skaf MS, Polikarpov I. An alternative conformation of ERβ bound to estradiol reveals H12 in a stable antagonist position. Sci Rep. 2017 Jun 14;7(1):3509.

[23] Matsui Y, Yamaguchi T, Yamazaki T, Yoshida M, Arai M, Terasaka N, et al. Discovery and structure-guided optimization of tert-butyl 6-(phenoxymethyl)-3-(trifluoromethyl)benzoates as liver X receptor agonists. Bioorganic & Medicinal Chemistry Letters. 2015 Sep;25(18):3914–20.

[24] Cheung J, Gary EN, Shiomi K, Rosenberry TL. Structures of Human Acetylcholinesterase Bound to Dihydrotanshinone I and Territrem B Show Peripheral Site Flexibility. ACS Med Chem Lett. 2013 Nov 14;4(11):1091–6.

[25] Viayna E, Coquelle N, Cieslikiewicz-Bouet M, Cisternas P, Oliva CA, Sánchez-López E, et al. Discovery of a Potent Dual Inhibitor of Acetylcholinesterase and Butyrylcholinesterase with Antioxidant Activity that Alleviates Alzheimer-like Pathology in Old APP/PS1 Mice. J Med Chem. 2021 Jan 14;64(1):812–39.

[26] Alterio V, Monti SM, Truppo E, Pedone C, Supuran CT, De Simone G. The first example of a significant active site conformational rearrangement in a carbonic anhydrase-inhibitor adduct: the carbonic anhydrase I–topiramate complex. Org Biomol Chem. 2010;8(15):3528.

[27] Temperini C, Cecchi A, Boyle NA, Scozzafava A, Cabeza JE, Wentworth P, et al. Carbonic anhydrase inhibitors. Interaction of 2-N,N-dimethylamino-1,3,4-thiadiazole-5-methanesulfonamide with 12 mammalian isoforms: Kinetic and X-ray crystallographic studies. Bioorganic & Medicinal Chemistry Letters. 2008 Feb;18(3):999–1005.

[28] Duda DM, Tu C, Fisher SZ, An H, Yoshioka C, Govindasamy L, et al. Human Carbonic Anhydrase III: Structural and Kinetic Study of Catalysis and Proton Transfer ·. Biochemistry. 2005 Aug 1;44(30):10046–53.

[29] Vernier W, Chong W, Rewolinski D, Greasley S, Pauly T, Shaw M, et al. Thioether benzenesulfonamide inhibitors of carbonic anhydrases II and IV: Structure-based drug design, synthesis, and biological evaluation. Bioorganic & Medicinal Chemistry. 2010 May;18(9):3307–19.

[30] Nocentini A, Alterio V, Bua S, Micheli L, Esposito D, Buonanno M, et al. Phenyl(thio)phosphon(amid)ate Benzenesulfonamides as Potent and Selective Inhibitors of Human Carbonic Anhydrases II and VII Counteract Allodynia in a Mouse Model of Oxaliplatin-Induced Neuropathy. J Med Chem. 2020 May 28;63(10):5185–200.

[31] Leitans J, Kazaks A, Balode A, Ivanova J, Zalubovskis R, Supuran CT, et al. Efficient Expression and Crystallization System of Cancer-Associated Carbonic Anhydrase Isoform IX. J Med Chem. 2015 Nov 25;58(22):9004–9.

[32] Dudutienė V, Zubrienė A, Smirnov A, Timm DD, Smirnovienė J, Kazokaitė J, et al. Functionalization of Fluorinated Benzenesulfonamides and Their Inhibitory Properties toward Carbonic Anhydrases. ChemMedChem. 2015 Apr;10(4):662–87.